Adsorption and self-assembly properties of the plant based biosurfactant, Glycyrrhizic acid.

IM Tucker[1], A Burley[1], RE Petkova[1], SL Hosking[1], J Penfold[2,3,†], RK Thomas[2], PX Li[3], JRP Webster[3], R Welbourn[3], J Doutch[3].

1. Unilever Research and Development, Port Sunlight Laboratory, Quarry Road East, Bebington, Wirral, UK
2. Physical and Theoretical Chemistry Laboratory, Oxford University, South Parks Road, Oxford, UK
3. ISIS Facility, STFC, Rutherford Appleton Laboratory, Harwell Campus, Didcot, OXON, UK

† Corresponding Author: Professor Jeff Penfold; phone: +44 1235 445681; email: jeff.penfold@stfc.ac.uk

Keywords: Saponin, Glycyrrhizic acid, adsorption, air-solution interface, neutron reflectivity, self-assembly, gelation, small angle neutron scattering

ABSTRACT

There is an increased interest in the use of natural surfactant as replacements for synthetic surfactants due to their biosustainable and biocompatible properties. A category of natural surfactants which are attracting much current interest is the triterpenoid saponins; surface active components found extensively in a wide range of plant species. A wide range of different saponin structures exist, depending upon the plant species they are extracted from; but regardless of the variation in structural details they are all highly surface active glycosides. Greater exploitation and application requires a characterisation and understanding of their basic adsorption and self-assembly properties.

Hypothesis

Glycyrrhizic acid, extracted from Licorice root, is a monodesmosidic triterpenoid saponin. It is widely used in cosmetic and pharmaceutical applications due to its anti-inflammatory properties, and is an ingredient in foods as a sweetener additive. It has an additional attraction due to its gel forming properties at relatively low concentrations. Although it has attracted much recent attention, many of its basic surface active characteristics, adsorption and self-assembly, remain relatively unexplored. How the structure of the Glycyrrhizic acid saponin affects its surface active properties and the impact of gelation on these properties are important considerations, and to investigate these are the focus of the study.

Experiments

In this paper the adsorption properties at the air-water interface and the self-assembly in solution have been investigated using by neutron reflectivity and small angle neutron scattering; in non-gelling and gelling conditions.

Findings

The adsorption isotherm is determined in water and in the presence of gelling additives, and compared with the adsorption behaviour of other saponins. Gelation has minimal impact on the adsorption; apart from producing a rougher surface with a surface texture on a macroscopic length scale. Globular micelles are formed in aqueous solution with modest anisotropy, and are compared with the structure of other saponin micelles. The addition of gelling agents results in only minimal micelle growth, and the solutions remain isotropic under applied shear flow.

INTRODUCTION

The use of natural surfactants as replacements for synthetic surfactants of mainly petrochemical origin are of increasing interest, due to their biocompatible and biosustainable properties (1-6). These may be derived directly from plant or animal origins, and can be used without further chemical synthesis (1), or involve further synthesis, or involve further synthesis via a bacterial route (5, 6). Although their interest and traditional application in detergency and medicines are long standing, the saponins are a class of biosurfactants that are attracting much current interest (7-11). This is chiefly because they are present in quantity in residual biomass from other food product sources which could in principle be harvested prior to disposal via the typical animal feed route with only minimal impact on their waste stream.

Saponins are highly surface active biosurfactants, glycosides, that are present in a wide range of different plant species (7-11). Their molecular structure is quite different to most synthetic surfactants. Their surface activity results from a hydrophobic component consisting mostly of a triterpenoid or steroid group and a hydrophilic region consisting of different saccharide groups, attached to the hydrophobic scaffold by glycoside bonds (7). The saccharide structure can be mono-, di-, or tri-desmosidic and contain one to three sugar groups, which are commonly glucose, galactose, rhamnose, arabinose, xylose or fructose. A wide range of structures and complexities in the structures arise from the wide range of plant species in which they exist, and this has given rise to a wide range of different physicochemical properties and biological activities (8).

In particular their surface activity (12-14) and the formation of highly viscoelastic surfaces (15-18) have resulted in an established use as an emulsifier and foam / bubble stabiliser in different foods and beverages (10, 11, 19-22). Saponins also exhibit a range of important biological properties and functions; such as anti-inflammatory, anti-fungal, anti-bacterial, anti-viral, anti-cancer and cholesterol lowering functions. This has resulted in applications in natural medicines (23-25), shampoos and cosmetics, and anti-ageing products (26).

The potential for an even broader and more mainstream range of applications of saponins requires a characterisation and understanding of their basic physicochemical properties, such as adsorption and self-assembly. This has resulted in a range of studies of the adsorption properties (12-18, 20, 27-30) and self-assembly behaviour (30-34) of different saponins; which has included escin, tea saponin and Quillaja saponins, and many others. Yet there remains much to investigate, and particularly for the Glycyrrhizic acid, GA, saponin, which is the subject of this study.

Glycyrrhizic acid is a monodesmosidic triterpenoid saponin, extracted from Licorice root (35). It is especially important in food formulations as a sweetener, as it is thirty times more effective than glucose (36). The reported chemical structure of GA, see figure 1, consists of a hydrophobic triterpenoid aglycon linked to a hydrophilic glycon consisting of two linked d-glycoronic acid groups (35). Apart from its

application in foods it has attracted much interest because of its biological activity (37). It has been widely used in cosmetics as a result of its anti-inflammatory properties (37, 38).

Although a range of studies have addressed some of the issues relating to GA adsorption and self-assembly (35-42), to pursue a greater range of potential applications a greater fundamental characterisation and understanding of the adsorption and self-assembly properties of GA is required. It has been previously demonstrated that neutron reflectivity, NR, and small angle neutron scattering, SANS, are powerful techniques for investigating surfactant adsorption (43) and self-assembly (44); and these techniques have been applied here to the study of GA adsorption at the air / water interface and in the formation of GA micelles in solution. NR has been shown previously to be effective in characterising saponin adsorption in a study of escin, tea saponin and Quillaja saponin adsorption at the air / water interface (12), and subsequently in the study of escin / sodium dodecyl sulfate, SDS, and escin / nonionic surfactant mixed adsorption (45, 46).

The adsorption isotherm of GA has been determined at the air / water interface using NR, and in the presence of gelling additives; and the adsorption properties are compared with those of other broadly related saponins. The effect of gelation and the additives on the adsorption is evaluated. The globular micelles formed by GA in solution are characterised by SANS and compared with the structure of some other saponin micellar structures. The impact of the gelling agents on the micelle structure and their response to shear flow are investigated.

EXPERIMENTAL DETAILS

(i) Neutron Reflectivity

The neutron reflectivity measurements at the air-solution interface were made on the INTER reflectometer (47) at the ISIS neutron source. The specular reflectivity measurements were made using a single detector and the off-specular measurements using a small area detector with a spatial resolution < 1 mm. The reflectivity, R(Q), was measured as a function of wave vector transfer, Q, perpendicular to the liquid surface, z direction. Q is defined as $Q=4\pi\sin\theta/\lambda$, where θ and λ are the grazing angle of incidence and the neutron wavelength. A Q range ~ 0.01 to 0.33 $Å^{-1}$ was covered using a λ range of 1.0 to 15 Å and two different angles of incidence of 0.8 and 2.3º. The reflectivity was normalised to an absolute scale by reference to the direct beam intensity and the reflectivity from a deuterium oxide, D_2O, surface. The measurements were made in sealed Teflon troughs containing ~ 25 mL of solution and maintained at 25ºC. The measurements were made sequentially on a 7 position sample changer. The measurement of each reflectivity profile (both angles of incidence) took ~ 40 to 60 minutes. Some repeated measurements were made to confirm equilibrium adsorption, and to probe the impact of gelation on the reflectivity and hence the adsorption.

In the kinematic or Born approximation (43) R(Q) is related to the square of the Fourier transform of the scattering length density profile, ρ(z),

$$R(Q) = \frac{16\pi^2}{Q^2}\left|\int \rho(z) e^{-iQz} dz\right|^2 \qquad (1)$$

where $\rho(z) = \sum_i b_i n_i(z)$, $n_i(z)$ is the number density distribution of the ith component and b_i is the scattering length. D and H have different scattering lengths (6.67×10^{-6} and -3.75×10^{-6} Å respectively), and so D/H isotopic labelling can be used to manipulate ρ(z). This is the basis of the exploitation of NR to study surfactant adsorption (43). In determining the adsorption and the surface structure of the adsorbed layer of surfactant at the air-water interface a contrast in the neuron refractive index (related to ρ(z)) is usually established by deuterium labelling the surfactant and using null reflecting water, nrw, (92 mol% H_2O / 8 mol% D_2O with a scattering length density of zero, the same as air). Deuterium labelling of the plant extracted saponins is not currently feasible, but the intrinsic contrast is sufficient ($\sum b = 1.4 \times 10^{-3}$ Å for GA saponin) to obtain a measurable and quantifiable reflectivity. In this study the consequences of low contrast have been minimised by using the capabilities of the INTER reflectometer to generate reflectivity data at a lower angle of incidence (0.8º), together with the increased neutron flux available at the ISIS Second Target Station. Consequently measurements on these materials have been relatively straightforward without significantly increased measurement times.

In these circumstances, assuming a single layer of uniform composition, the neutron reflectivity can be written exactly as,

$$R = \frac{16\pi^2}{Q^4}(2\rho)^2 \sin\left(\frac{Qd}{2}\right)^2 \qquad (2)$$

where d and ρ are the thickness and scattering length density of the adsorbed layer, and the adsorbed amount, Γ, is given by,

$$\Gamma = d\rho / N_a \sum b \qquad (3)$$

where N_a is Avogadro's number, and the area / molecule, A, is $A = 1/N_a\Gamma$.

(ii) Small angle neutron scattering

The SANS measurements were made on the SANS2D diffractometer (48) at the ISIS neutron source using the 'white beam time of flight' method. The scattered intensity, I(Q), was measured over a Q range of ~ 0.006 to 0.5 $Å^{-1}$, using a sample to detector distance of 4 m, a neutron wavelength range of 2 to 12 Å, and a beam diameter of 12 mm. The solutions were contained in 2 mm path length quartz cells and maintained at 25ºC. Measurements were also made using a Couette shear flow cell (49, 50),

using a 8 mm diameter beam, and with the neutron beam incident orthogonal to the vorticity – shear flow plane, for shear rates up to 15,000 s^{-1} (49, 50). The scattering from the cells and solvent (D_2O) were subtracted from the data, and the data were normalised to detector response and the spectral distribution of the incident beam using standard procedures (51).

The SANS data for the globular micelle structures was modelled using a standard model for interacting globular polydisperse micelles, where in the 'decoupling approximation' (52) the scattered intensity I(Q) is written as,

$$I(Q) = n\left[S(Q)\left|\langle F(Q)\rangle_Q\right|^2 + \left\langle \left|F(Q)\right|^2 \right\rangle_Q - \left|\langle F(Q)\rangle_Q\right|^2 \right] \qquad (4)$$

where <*Q*> denotes averages over particles size and orientation (where the decoupling approximation assumes no correlation in position, size, and orientation), *n* is the micelle number density, *S*(*Q*) the structure factor, and *F*(*Q*) the form factor. The form factor used is a standard core-shell micelle model (52), described in more detail later, and S(Q) describes the inter-micellar interactions using a rescaled mean spherical approximation, RMSA, calculation (53) for a repulsive screened Coulombic / hard core potential.

(iii) Materials

The Glycyrrchizic acid, GA, was obtained from SIGMA, in the form of the ammonium salt with a purity of > 97%, and was used as supplied. The GA has a molecular formula of $C_{42}H_{62}O_{16}$, and a MW of 822 gm / mol.

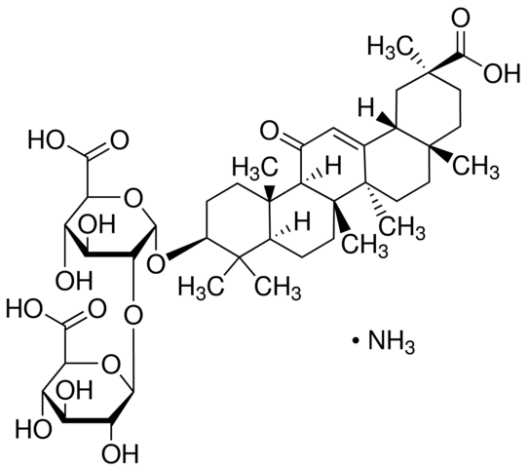

Figure 1. *Molecular structure of Glycyrrchizic acid*

GA is predominantly a mixture of the α- and β- isomeric forms (35, 38), and shown in the figure is the α- isomer. The NR measurements were made in nrw and the SANS measurements in D_2O. The formation of clear rigid gels of GA occur if the solutions are heated to 45ºC and allowed to cool to room temperature. In the measurements reported here the solutions were heated to a temperature exceeding

45ºC in an ultrasonic bath for 30 minutes. The NR and SANS measurements were made on solutions that had not gelled, unless otherwise stated. Without the addition of buffer, dissolution in aqueous solution at the concentrations used resulted in a measured pH ~ 4 to 5. In this pH range the carboxyl groups will be protonated and the surfactant is expected to be predominantly nonionic.

NR measurements were also made using a freeze dried sample in which the main impurity, ammonium acetate, is largely removed. The purity of the GA sample was measured by LC-MS, liquid chromatography mass spectrometry, before and after freeze drying, and the ammonium nitrate initially present was removed.

At lower pH values the low degree of dissociation of the carbonyl groups result in a lower solubility. At high pH, >6, the carbonyl groups are expected to be fully dissociated and the solubility is correspondingly higher. The change in solubility and hence solution activity gives rise to a change in the bulk aggregate formation and the tendency towards gelation. This results in difficulties and variations in the surface tension, ST, as discussed further later in the paper. Hence no ST data are included in this paper and NR alone is used to determine the surface activity.

The addition of electrolyte and the reduction of pH induces gelation more readily, reducing the time for gelation to occur from hours to minutes. Further NR and SANS measurements were made with the addition of NaCl, $MgCl_2$, Na_2SO_4, $AlCl_3$, and citric acid, in order to promote gelation and to study the impact of different electrolytes with increasing valence from mono to di to trivalent. The addition of $AlCl_3$ and citric acid result in a reduction in solution pH, and was specifically measured for the addition of 0.1 mM $AlCl_3$ to be < 4.0.

The reagents used were all obtained from SIGMA at analytical grade (>99,9% purity), and the D_2O (>99,9% purity) was also obtained from SIGMA. High purity water (resistivity ~ 18.2 MΩcm) was used throughout. All glassware, Teflon troughs, quartz sample cells, used in the NR and SANS measurements and in the sample preparation, were cleaned in alkali detergent (Decon90) and extensively rinsed in high purity water.

For comparison with the GA SANS data, SANS measurements were made for 5, 10, 25 mM escin, 25 mM tea saponin and 25 mM *Quillaja* saponin, all in 0.1 M NaCl, amd under the same conditions as described earlier for the GA solutions. The escin was obtained from SIGMA (Cas. No. 6805-41-0, batch no BLV8469V-2, 95% purity) it was used as supplied, and was from the same batch as for the results reported in reference 12. The *Quillaja* saponin, *Quillaja Bark Saponin*, was obtained from SIGMA, and used as supplied with a purity ~ 30%. The tea saponin, *Camelia Oleifera Able Tea saponin*, was obtained from Nanjing Zelang Medical Technology Co. Ltd., China (supplied through Zhejiang Yuhung Import and Export Co. Ltd.) with 96% purity, was used as supplied, and is the same source as used in reference 12. The structures of those saponins are shown in figure S1 in the Supporting Information.

The strength of the gels formed was measured separately using Light Scattering Microrheometry (54). Little variation in the elastic moduli or in the crossover point of G' / G" (storage and loss moduli) of the gels formed under the different conditions explored.

RESULTS and DISCUSSION

(a) Surface adsorption of GA

NR was used to measure the adsorption isotherm of GA at the air-water interface in the concentration range 0.04 to 4 mM. The data are well described by a single layer of uniform composition, as shown in figure S2 in the Supporting Information. The thickness of the adsorbed layer was determined using equation 2 and the adsorbed amount using equations 2 and 3. The optimal thickness of the adsorbed layer is 35±3 Å, as illustrated in figure S3 and tabulated in table S1 in the Supporting Information. In figure S3 the χ^2 (goodness of fit) parameter is plotted versus thickness for 1.25mM GA, in the region of saturation adsorption, and gives an optimal thickness of 35 Å. This compares with a thickness of 28 and 30 Å reported for the escin and tea saponins (12). Escin is a monodesmosodic saponin with a similar structure to GA, except that escin has three rather than the two saccharide groups of GA. A more detailed structural analysis of the escin adsorbed layer (12) indicated that its hydrophilic region was closely packed and that the hydrophobic portion was tilted. Furthermore it showed that the packing at saturation was dominated by the hydrophilic region and that the hydrophobic region played a more secondary role. The increased thickness of the GA adsorbed layer suggests that the hydrophobic portion is not tilted, unlike the escin molecule. However there is a greater uncertainty in the value of the GA layer thickness as the $\sum b$ value for GA (1.4×10^{-3} Å) is lower than that of escin and the tea saponin ($\sum b \sim 2.0 \times 10^{-3}$ Å), and significantly lower than most deuterium labelled conventional synthetic surfactants where the $\sum b$ is typically in the range 2.5 to 3.5 x 10^{-3} Å. For this reason a more detailed structural investigation was not pursued at this stage. This low value of the $\sum b$ will also impact upon the uncertainty in the determination of the adsorbed amount, which is discussed in the following paragraph.

In the determination of the adsorbed amount, as demonstrated in equation 3, it is the product $d.\rho$ that is important, and so the individual uncertainties in d and ρ are less important. At these relatively low coverages and in the Q range explored in the NR measurements a range of d values will generally fit the data and the values of ρ will vary inversely with d to exactly compensate (43). The adsorption isotherm for GA in water is shown in figure 2. To obtain a greater understanding of the reproducibility of the data and the associated errors, in light of the small $\sum b$ value for GA, the adsorption isotherm was measured separately using two different allocations of beam time. The results shown in figure 2 indicate that the data are within error reproducible, and that the mean saturated adsorbed amount is 1.85 ±0.15 x 10^{-10} mol cm^{-2}. Measurements were also made on a freeze dried sample, and are also shown in the figure.

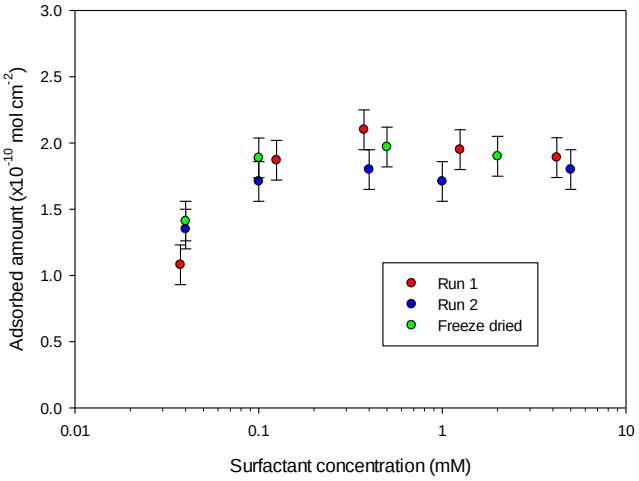

Figure 2. *Adsorption isotherms for GA, see legend for details. The data are available in table S2 in the Supporting Information.*

Freeze drying results in the removal of the main impurity in the GA sample, ammonium acetate. The adsorption isotherm for the freeze dried sample is within error the same as the sample prior to freeze drying, and indicates that the ammonium acetate impurity is relatively low or that it has little impact upon the adsorption. The general form of the isotherms are broadly similar to those reported for escin (12), and similar to that reported for nonionic surfactants (43). That is, above the nominal critical micelle concentration, cmc, the adsorption reaches a plateau value (55, 56). Whereas for ionic surfactants the adsorption in general continues to increase (56). As discussed earlier, it would be expected that the GA saponin is essentially nonionic at the pH of the measurements, or at least only weakly anionic. The results from GA are consistent with what was observed for escin at pH 4 to 8 (12), where the NR and surface tension, ST, data were in good agreement on the basis of the adsorbed layer being uncharged.

Given that for nonionic surfactants saturation adsorption is reached at or before the cmc is reached (54), from the isotherms in figure 2 the cmc for GA is estimated to be ≥ 0.1 mM. This is broadly consistent with the observations and correlation between the NR derived isotherms and ST determined cmc values for escin, reported by Penfold et al (12). Kondo et al (38) reported significant and similar surface activities for α- and β- glycyrrhizin, on the basis of ST data. Their ST data did not show a well-defined break point, and cmc values were not quoted in the paper. However, taking into account the uncertainty is defining the cmc from that data, it is in the range 0.1 to 1 mM. Matsuoka et al (39) reported a low solubility at very low pH, which increases markedly for pH > 4. From ST they determined a cmc which was strongly pH dependent, ranging from 2.5 to 5.5 mM, depending upon the pH and method used. Furthermore they determined the adsorbed amount using the Gibbs equation, which varied from 1.3x10^{-}

^{10} mol cm^{-2} at pH 5 to 2.9 x 10^{-10} mol cm^{-2} at pH 6. Given the variance in the ST data in determining the cmc and adsorbed amounts for GA from Kondo et al (38) and Matsuoka et al (39) no ST data are presented here. As will be demonstrated later, the onset of gelation results in a strongly viscoelastic surface with structure on a macroscopic distance scale. These effects will dominate ST measurements and introduce large uncertainties and measurement difficulties. It is quite difficult to stop GA from forming gels and it was observed in several measurements that a rigid surface layer formed. However the adsorbed amount was within error unchanged, as is shown specifically later in this paper. As a non-invasive surface probe NR is relatively unaffected by this phenomena. It is assumed here that the NR data provides a more reliable determination of the adsorption (54, 55). The NR deduced cmc, between 0.1 and 1 mM, is consistent with the data from Kondo et al (38), but significantly less than the values reported by Matsuoka et al (39) of 2.9 and 5.4 mM at pH 5 and 6. Figure S4 in the Supporting Information shows a comparison of the GA isotherm (taken as the average of the data in figure 2) with NR data previously reported for escin at pH 4 (12). Apart from the increase in the saturation adsorption values for escin compared to the GA saponin, the isotherms are remarkably similar. Taking into account the agreement between NR and ST data for escin (12), from the NR data in figures 2 and S4 in the Supporting Information the cmc for the GA saponin is ~ 0.1 mM.

The saturation adsorption for GA reported here, ~ 1.85 ±0.15 x 10^{-10} mol cm^{-2}, is significantly different those reported by Matsuoka et al (39) at pH 5 and 6. However the data of Matsuoka et al (39) is derived from ST data, and for a different source of GA. The divergence in values compared to the date measured here may be associated with the uncertainties and difficulties associated with the ST measurement for GA or due to the particular saponin source and purity, which was not quoted by Matsuoka et al (39).

The value determined here, 1.85x10^{-10} mol cm^{-2}, compares with the values reported by Penfold et al (12) for escin of 2.4 x10^{-10} mol cm^{-2} (which was within error independent of pH), for tea saponin of 2.1 x10^{-10} mol cm^{-2}, and for the Quillaja saponin of 1.9x10^{-10} mol cm^{-2}. The escin and GA saponins have similar molecular structures, with similar hydrophobic scaffolds. Escin has three saccharide groups with a single carboxyl group, and GA has two saccharide groups and three carboxyl groups. Both saponins at the pH of the measurements are nonionic or only weakly anionic. Hence it is interesting and unexpected that the saturation adsorption for GA is significantly lower than that of escin. Penfold et al (12), in a detailed NR study of the structure of the escin adsorbed layer, illustrated that the limiting packing was determined by the saccharide groups and their interactions, and that the hydrophobic scaffold plays a more secondary role. Hence it is assumed here that the reduced saturation adsorption of GA is associated with the greater number of carboxyl groups, even though there is a smaller number of saccharide groups. In contrast the lower saturation adsorption of the tea and Quillaja saponins are more readily explained by the greater number of saccharide groups for the tea saponin and the bidesmosidic structure of the Quillaja saponin. Further structural studies at the air-water interface using

partial deuterium labelling would be required to resolve this question, and as discussed earlier is not currently practicable.

(b) Influence of electrolyte and gelation on adsorption

At higher GA concentrations and at low pH GA has a tendency to form clear gels (38), due to the formation of rod-like micelles or fibrillar structures (34, 38, 39). The tendency to gel is enhanced in the presence of additives such as NaCl, $MgCl_2$, $AlCl_3$ and citric acid. NR has been used to investigate the extent to which additives affect the adsorption at the air-water interface, and how actual gel formation affects the measured reflectivity. The range of additives chosen here enable the impact of pH and different valence electrolytes, from mono to trivalent, on the nature of the adsorption to be probed.

Figure 3 shows a comparison of the adsorption isotherms of GA, GA / 50 mM NaCl, GA / 1 mM $MgCl_2$, GA / 0.2 mM $AlCl_3$ and GA / I mM citric acid.

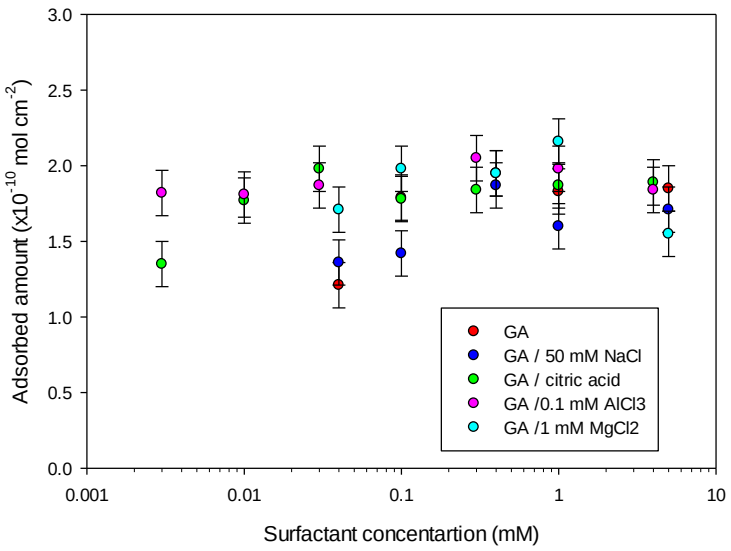

Figure 3. *Adsorption isotherm for GA, GA / 50 mM NaCl, Ga / 1 mM $MgCl_2$, GA / 0.2 mM $AlCl_3$ and GA / I mM citric acid: see legend for details. The data are available in table S4 in the Supporting Information.*

Within experimental error the saturation adsorption values for GA with the different additives are the same as for GA in the absence of the additive. Furthermore the addition of 50 mM NaCl results in an isotherm that is close to that of GA in the absence of electrolyte. For the addition of 0.1 mM $AlCl_3$ and 1 mM citric acid and to a lesser extent 1 mM $MgCl_2$ the adsorption plateau extends to a significantly lower concentration. This implies a significant reduction in the cmc. It is important to note (53) that at the very low concentrations measured, between 10^{-5} and 10^{-6} M, depletion effects will start to have an impact.

It is well known that the addition of electrolyte will significantly reduce the cmc of ionic surfactants (57), and that multivalent electrolytes, such as $MgCl_2$ and $AlCl_3$, have an even greater impact and are more effective in reducing cmc values (58). However, given that the evidence presented earlier implies that GA is nonionic and at best only weakly ionic, the extent of the impact of electrolyte on the reduction in the cmc is unexpected. This is further compounded by the observation that the saturation adsorption is unaffected by the addition of electrolyte. It was previously observed for escin (12) that a decrease in pH from 8 to 4 resulted in a significant reduction in the cmc, but resulted in no change in the saturation adsorption values. In that case it was argued that charge had little effect on the packing at saturation, but affected the surface activity at lower concentrations. The addition of 1 mM citric acid, 0.2 mM $AlCl_3$ and 1 mM $MgCl_2$ result in a reduction in the pH; and for 0.2 mM $AlCl_3$ the pH is < 4. Hence the impact on the cmc is similar to that observed for escin with pH (12). For GA this apparent and significant decrease in the effective cmc also cannot be charge mitigated, and the onset of micellisation must be more readily promoted by improved packing and reduction in inter-molecular interactions which do not impact upon the saturation adsorption. However, given that it occurs for $MgCl_2$, $AlCl_3$, and citric acid, but not for NaCl, it also implies a specific interaction. These observations are broadly in common with those for escin (12). It is assumed here that the close proximity of the three carboxyl groups limits deprotonation and promotes the stronger interaction with the multivalent counterions. An alternative explanation is that the saturation adsorption could now occur well before the onset of micellisation.

With increasing time in the Teflon troughs used for the NR measurements, the GA solutions in the higher concentration range and especially in the presence of additives will tend to gel. NR measurements were made at increasing time intervals to explore the impact of gelation on the adsorption, the reflectivity and its interpretation in terms of the adsorbed amount. Figure S5 in the Supporting Information shows the time dependent adsorption for 5 mM GA and 5 mM GA / 50 mM NaCl, and the corresponding data are shown in table S5 in the Supporting Information. The measurements were made over a period of up to 1200 minutes after the solutions were initially established in the troughs. The results show that within experimental error the adsorbed amounts is invariant with time and gel formation, and so gel formation in the bulk solution does not appear to deplete surfactant from the surface.

The onset of gelation might also be expected to result in another mechanism which could be interpreted as a decrease in the adsorption. It might be expected that as the gel forms the surface will become rougher, and that the surface roughness would result in a decrease in the specular reflectivity and an increase in the off-specular scattering. In order to evaluate this some limited additional measurements were made, where the single detector on INTER was replaced by a linear position sensitive detector mounted in the vertical plane. In this geometry, in addition to measuring the reflectivity in the Q_z direction perpendicular to the surface plane, the Q_x component, the component in the surface plane, of

surface scattering is measured. This is shown in figure S6 in the Supporting Information for 5mM GA and 5mM GA / 1mM $MgCl_2$, where the uncorrected data are shown plotted as a function of scattering angle and neutron wavelength.

The horizontal band in figures S6 a and b in the Supporting Information is the specular ridge, measured at an angle of incidence of 0.8º, and gives a relatively sharp well defined specular signal and evidence of weak off-specular scattering adjacent to the specular ridge. A more quantitative evaluation of the scattering is presented in figure 4, where the scattered intensity is plotted versus Q_x, for data integrated over the Q_z range 0.02 to 0.06 $Å^{-1}$, for the same two samples as shown in figure S6 in the Supporting Information.

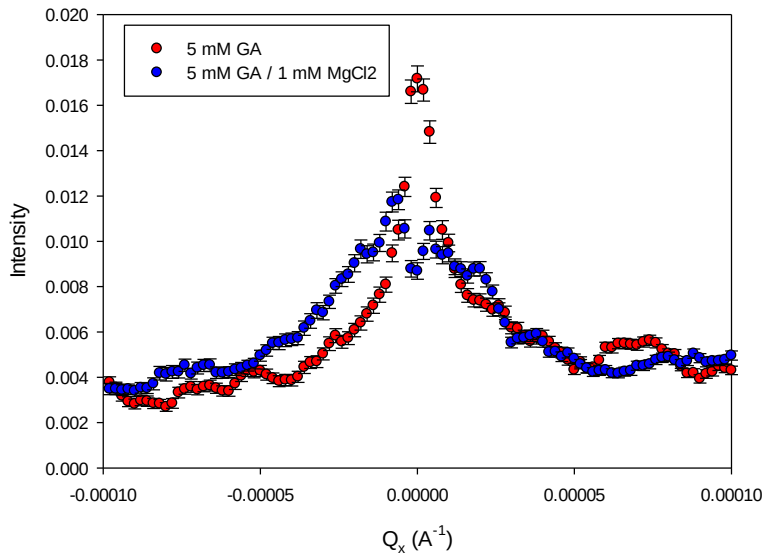

Figure 4. *Scattered Intensity versus Q_x, integrated over the Q_z range 0.02 to 0.06 $Å^{-1}$, for (red) 5 mM GA, (blue) 5 mM GA / 1 mM $MgCl_2$; see legend for details.*

The data in figure 6 highlights the main features of the impact of gelation on the surface scattering. Gelation, going from 5 mM GA to 5 mM GA / 1 mM $MgCl_2$, results in a broadening of the specular ridge and an increase in the scattered intensity in the wings of the distributions. Measuring the half widths of the distributions, ΔQ_x, in figure 4 shows an increase from $2.5 \pm 0.5 \times 10^{-4}$ $Å^{-1}$ to $4.5 \pm 0.5 \times 10^{-4}$ $Å^{-1}$. The impact of an increasingly roughened surface on the reflectivity will depend upon the length scale of the roughness features. If the in-plane length scale of the roughness is small compared to the neutron coherence length (≤ 1 μm) then the roughness will result in a reflectivity signal that falls off at a greater rate than Q^{-4} and will result in the appearance of structured or unstructured off-specular scattering. If the length scale of the roughness is large compared to the coherence length then the surface will appear rough on a macroscopic scale; that is, wavy. This will contribute to a broadening of the specular peak, like an additional instrumental resolution term. The data in figures S6 in the Supporting Information and figure 4 are consistent with an increasingly wavy surface on gelation, as quantified by

the increase in ΔQ_x. The invariance in the adsorption with time, in figure 4, then arises because the broadening of the specular signal still lies mainly within the detector acceptance solid angle and its associated collimation.

(c) **Self-assembly of GA in dilute solution**.

There has been much discussion about the nature of self-assembly in saponins (31, 33, 34), and especially the GA saponins (35, 39, 59). Here SANS has been used to investigate and characterise the micelle formation of GA in the concentration range 1 to 5 mM, and at a surfactant concentration of 5 mM in the presence of 50 mM NaCl, 1 mM $MgCl_2$, and 1 mM citric acid, The SANS data and model fits are shown in figure 5, and the associated key model parameters are summarised in table 1.

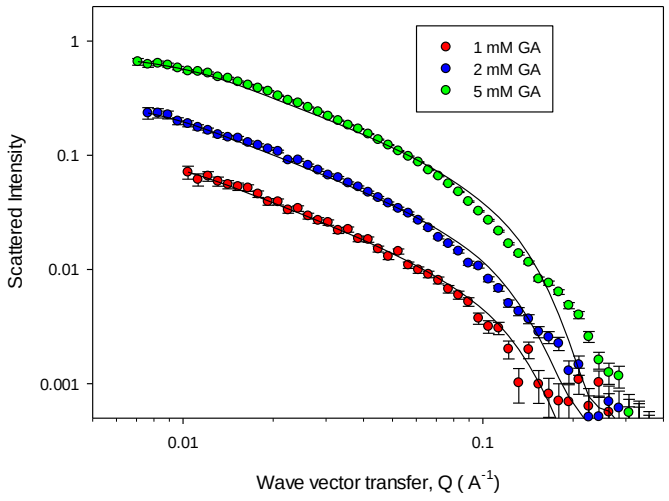

(a)

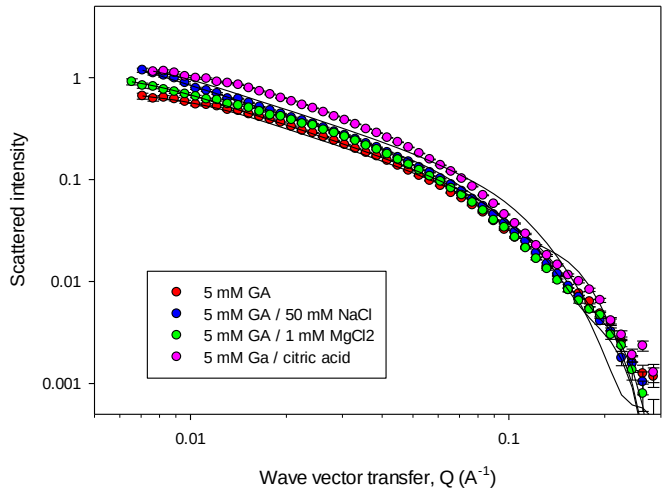

(b)

Figure 5. *Scattered Intensity versus wave vector transfer, Q, for (a) 1, 2, and 5 mM GA in D_2O, ad (b) 5 mM GA in 50 mM NaCl, 1 mM $MgCl_2$ and I mM citric acid; see legend for details. The solid lines are model calculations, as described in the text, and for the key model parameters summarised in table 1*

Sample	**R_1 (±1 Å)**	**R_2 (±1 Å)**	**ee (±2)**	**Aggregation number, ν (±20)**
1 mM GA	14	16	17	160
2 mM GA	14	16	19	170
5 mM GA	14	16	15	140
5 mM GA/50 mM NaCl	14	16	33	360
5 mM GA/1mM $MgCl_2$	14	16	21	200
5 mM GA/ 1 mM citric acid	14	16	20	190
5 mM escin / 0.1 M NaCl	20	25	7	200
10 mM escin / 0.1 M NaCl	20	25	11	320
25 mM escin / 0.1 M NaCl	20	25	24	670
25 mM Tea saponin/ 0.1M NaCl	20	25	6.5±0.5	67±5
25 mM Quillaja saponin/ 0.1M NaCl	15	17	2.2±0.5	25±2

Table 1. *Key model parameters from the analysis of the SANS data in figure 7 and 8.*

The SANS data for 1, 2 and 5 mM GA are shown in figure 5a and are consistent with elongated globular micellar solutions. The solid lines are model fits to the data using a core-shell prolate ellipsoid model, as described in detail elsewhere (44, 52, 53). The inner core contains the hydrophobic portion of GA with a dimension R_1 and an ellipticity ee, and the outer shell, R_2, contains the saccharide groups and associated hydration. The aggregation number is calculated assuming space filling within the elongated geometry. The key model parameters are summarised in table 1. Within experimental error the key parameters do not vary over this concentration range; R1 and R2 are 14 and 16 Å, the ellipticity ee is 17±2, and the aggregation number is 150±20. The ellipticity corresponds to a micelle length ~ 270 Å. Hence the micelle size is largely invariant over this concentration range. The prolate ellipse model is used here rather than a cylindrical form factor, as a single model can then be used to follow the evolution

in anisotropy in such systems. Furthermore in this size regime, when polydispersity is considered the differences in the respective form factors are not significant.

The SANS data in figure 5b shows the data for 5 mM GA and 5mM GA in 50 mM NaCl, 1 mM $MgCl_2$, and in 1 mM citric acid. The addition of electrolyte and citric acid results in a more elongated structure. In citric acid and 1 mM $MgCl_2$ the increase in micelle size is relatively modest; with an aggregation number increasing from ~150 to ~200, and an ellipticity increasing from ~17 to ~20. In 50 mM NaCl the micellar growth is more substantial; with an aggregation number ~ 350 and an ellipticity ~ 33. The addition of electrolyte results in micellar growth, from ~270 to ~360 Å in 1 mM $MgCl_2$ and to ~530 Å in 50 mM NaCl.

Predominantly the GA micelles, in the absence and presence of electrolyte, are elongated rod-like structures; and the addition of electrolyte promotes modest micelle growth. The micelle form factor dominates the scattering profile, and there is no clear evidence of a contribution from the inter-micellar, S(Q), interaction, as would be expected for a purely hardsphere interaction for essentially nonionic micelles at these relatively low volume fractions. Although micelle growth from globular towards more elongated structures is expected for ionic surfactants with the addition of electrolyte (57, 58), the evidence from the adsorption data is that GA is essentially nonionic. Hence it is assumed that the micelle growth observed here is associated with a reduction in headgroup interactions and improved packing that is not primarily electrostatic, as discussed earlier in the context of the cmc reduction in the presence of electrolyte.

The extent to which the saponin structure, and in particular the headgroup structure, affects the self-assembly is further explored here. Some preliminary SANS measurements were made for the escin, tea and Quillaja saponins, for direct comparison with the GA SANS data. Measurements were made for 5, 10, and 25 mM escin in 0.1 M NaCl and 25 mM tea and Quillaja sponins in 0.1M NaCl, and the data are shown in figure 6.

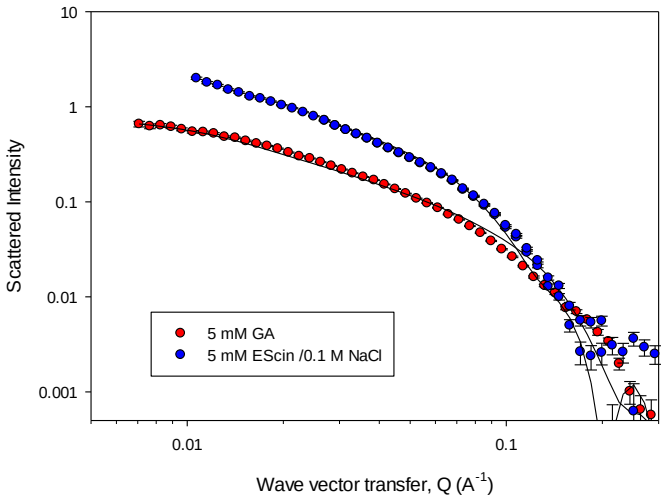

(a)

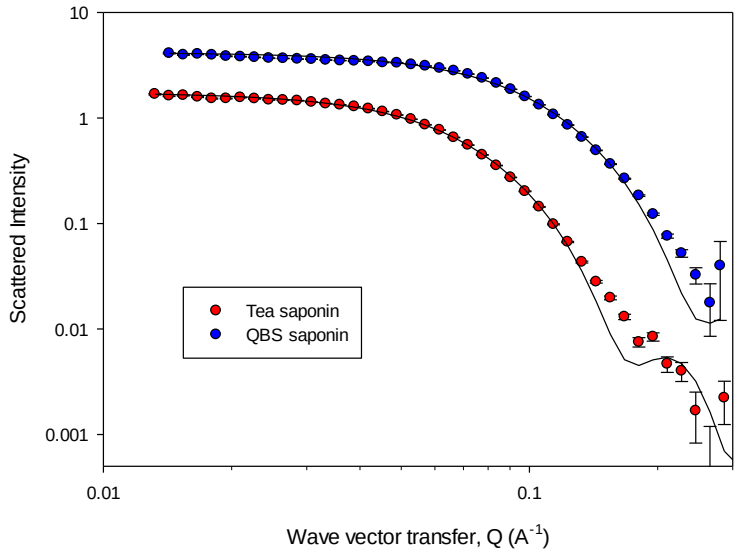

(b)

Figure 6. *Scattered Intensity versus Q for (a) 5, 10, 25 mM escin / 0.1 M NaCl in D_2O, (b) 25 mM tea and Quillaja saponins / 0.1M NaCl in D_2O; see legends for details. The solid lines are model calculations using the key model parameters in table 1 and for the model described in the text.*

The data in figure 6a for escin are consistent with elongated micelle structures, and the changes in the data reflect the increasing escin concentration and some micellar growth with concentration. The data are well described by the same elongated micelle model as used for the GA saponins, but with different structural parameters, see table 1. The micelle anisotropy in shape and aggregation numbers are larger: the ellipticity varies from ~ 7 to 24 and the aggregation number from ~200 to 700. Furthermore changes in the packing of the hydrophobic portion results in a larger short dimension of the ellipse, with R_1~ 20 Å and R_2 ~ 25 Å. The overall length of the elongated structures is now ~ 250 to 500 Å. The data in figure 6b are for 25 mM tea saponin and the Quillaja saponin, both in 0.1M NaCl. The scattering from these two micellar structures is quite different to those seen for the GA and escin saponins, and are consistent with relatively small globular micelles. Furthermore again there is an absence of a contribution from inter-micellar interactions, S(Q), which at these relatively low volume fractions of micelles would arise from charge interactions as the hard sphere contribution is small. Hence this implies that the micelles are essentially uncharged. The key model parameters are summarised in table 1. The parameters for the Quillaja saponin indicate a relatively small micelle, with an aggregation number ~ 25 and an ellipticity ~ 2.0. The core-shell dimensions are similar to those of GA, with R_1~15 and R_2~17 Å. The tea saponin micelles are also relatively small and globular, with an aggregation number ~ 70 and an elliptiicty ~6. In this case the core-shell parameters are similar to those of escin.

The SANS results presented here for GA, escin and the Quillaja saponins are broadly consistent with those reported in the literature from a limited range of studies. However the comparison is limited as some measurements are in electrolyte and at different surfactant concentrations, and information about the extent to which concentration and electrolyte impact upon micelle size in such systems is limited.

Matsuoka et al (39) used SAXS to characterise GA micelles and elongated rod-like structures with a radius ~ 15 Å and a length ~ 210 Å. Ralla et al (41) reported rod-like or fibrillary structures for GA, but no detailed quantitative parameters were presented. The focus of the work of Oliveria et al (59) was on the co-micellisation of GA saponins with a pluronic triblock copolymer, F127, and it is difficult to make a direct comparison with the quoted hydrodynamic radii.

Dargel et al (34), from SAXS data, report rod-like structures for escin, with R_g~ 31 Å and rod dimensions, diameter and length, ~ 30 and 100 Å. The results of Dargel et al (34) are not entirely consistent with the data in figure 6 and table 1 for escin. In the data presented here the escin micelles are significantly larger than the size quoted by Dargel et al. This discrepancy arises from the impact of NaCl on the micelle size.

The tea and Quillaja saponins, see figure 6b, both have significantly smaller micellar structures. The results for Quillaja saponin compare with values in the literature, where the structure of the Quillaja micelles have been more extensively explored than for other saponins (30, 31, 33), but show some variability. Mitra and Duggan (31) report from dynamic light scattering, DLS, aggregation numbers ~ 30 to 40 at room temperature, and which increase significantly with increasing temperature and concentration. This is consistent with the results of Oakenfull (31) who observed small globular micelles with an aggregation ~ 50 for Quillaja micelles. However Tippel et al (30) report hydrodynamic radii, from DLS measurements, varying from 65 to 120 Å. The data presented here are broadly consistent with that previously reported. Comparison between the data in the literature and that presented here suggest that electrolyte has little impact upon micelle structure.

Comparing the results in table 1 and figures 5 and 6 for GA and escin, the solution structures are broadly similar in that in both cases elongated structures occur, but the escin micelles are significantly larger than GA micelles in part because the escin data are in the presence of 0.1M NaCl. In the presence of electrolyte the GA micelles are much closer in size to the escin micelles, and when the impact of electrolyte and concentration are taken into account they are broadly similar. However there is a notable difference in the radius or short dimension of the elongated structures, where R1 and R2 increase from 14 / 16 Å for GA to 20 / 25 Å for escin. Although the molecular structures are broadly similar, as discussed earlier in that they have a similar hydrophobic portion and that escin has an extra saccharide group but one less carboxyl group in the hydrophilic region, the impact on the internal micelle packing is significant. In contrast, the significantly larger headgroup structure for the tea saponin with 4 saccharide groups and for the Quillaja saponin with the bidesmosidic structure results in a greater

preferred curvature. Hence for both the tea and Quillaja saponins smaller more globular micelles structures occur. In the self-assembly of surfactants with more conventional structures the evolution in micelle size is well described by the simple packing criteria encapsulated by Israelachvili, Mitchell, and Ninham (60). Here the same criteria are broadly qualitatively consistent, but the comparison of the GA and escin micelle parameters presented here suggest that the packing requirements are more complex.

The implication from recent studies (38, 39, 41, 42) is that the gel formation in GA solutions is associated with fibril formation. The SANS results presented here show only relatively modest micellar growth in the presence of NaCl, $MgCl_2$ and citric acid, all additives which promote gel formation. To explore this further some additional SANS measurements were made under shear flow. The measurements were made in a Couette shear flow cell (49, 50) in which the neutron beam was incident orthogonal to the shear flow-vorticity plane, at shear rates of up to 15,000 s^{-1} for 5 mM GA / 1 mM $MgCl_2$ in D_2O. In this scattering geometry the alignment of ansiotropically shaped micelles will result in an anisotropic scattering pattern (49, 50), consistent with alignment in the flow direction. The normalised 2-D scattering patterns at zero flow and 15,000 sec^{-1} are shown in figure 7, and are representative of the patterns measured over that shear rate range.

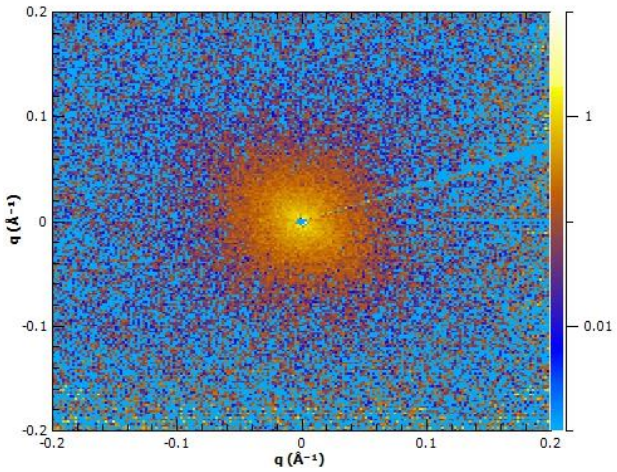

(a)

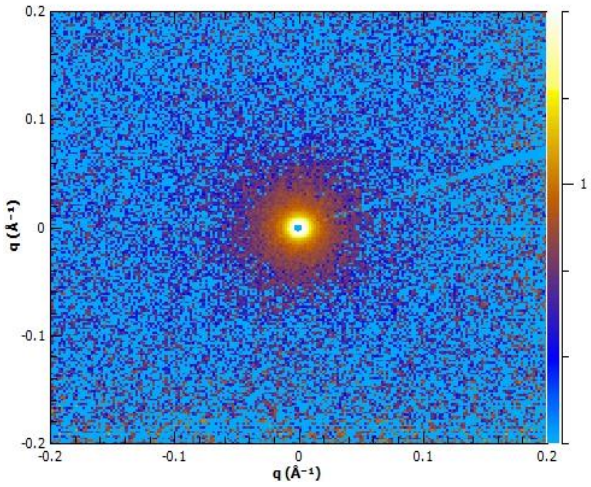

(b)

Figure 7. *Scattering patterns for 5 mM GA / 1 mM $MgCl_2$ / D_2O, (a) zero shear, (b) 15,000 sec^{-1}; see legend for details.*

The results show that the scattering patterns are symmetrical at zero shear and at higher shear rates. These patterns are consistent with the modest anisotropies determined from the static SANS measurements for GA, see figure 5 and table 1. Furthermore the flow data implies also that significant micellar growth is not induced by shear flow. It has been implied that the formation of rod-like micelles or fibrillary structures (41) are responsible for the gelling properties. However the data indicate that there are no significantly longer fibrillary type structures present or that they are at undetectably low concentrations. The origins of the observed gel formation therefore lies in the larger 3-D network formed by these elliptical structures, which are easily disrupted by modest shear.

(d) Correlation between surface and solution behaviour

There is some overlap between the concentration ranges explored in the surface adsorption measurements and in the determination of the solution self-assembly structures, and so the potential for correlations between the two phenomena is discussed in more detail.

Above the cmc the adsorption remains constant with increasing concentration, and this is characteristic of a nonionic or weakly ionic species at the interface as discussed previously by Li et al (55) and Xu et al (56) for more conventional surfactants. It is also consistent with previous measurements for the saponin escin (12). The saturation adsorption is also unaffected by the addition of electrolyte, reinforcing the inference that the adsorbed species is only weakly ionic. The SANS data indicate elongated micellar structures in solution in the concentration range 1 to 5 mM which are independent of concentration. The data also show no indication of the micelles being highly charged, and so in that respect are consistent with the surface adsorption trends. However the addition of electrolyte does

promote micellar growth and promote the onset of saturation adsorption at lower concentrations. The results suggest that reducing pH and the associated deprotonation of the carboxyl groups in GA, and the specific interaction with the different cations modifies the micelle packing to promote micellisation and micellar growth. It is not, however, manifest in changes in the saturation adsorption. It was shown in a more detailed structural study of the adsorption of the escin and tea saponins (12) that the adsorbed structure at saturation is already dominated by the close packing of the saccharide groups, such that there is little scope for further increases in the packing density at the interface.

CONCLUSIONS

NR and SANS have been used to characterise the adsorption and self-assembly properties of the saponin Glycryrrhizic acid. The results provide a sound basis upon which to explore the wider physico-chemical properties and a wider portfolio of potential applications and interactions.

The nature of the adsorption at the air-water interface is compared with the adsorption of other well characterised saponin molecules. The adsorption isotherm resembles that of a nonionic surfactant (54), similar to that encountered with escin (12). The saturation adsorption value is lower than for escin, Quillaja and tea saponins (12), and imply that the apart from the number of saccharide groups and their structural arrangement the number of carboxyl groups imposes further constraints on the packing at the interface. This is also highlighted in the measured adsorbed layer thickness, which is greater than for the escin and tea saponins. This implies some greater vertical disorder in the packing and a less tilted geometry compared to that reported for escin (12); and is an area for future more detailed investigations. The form of the adsorption isotherm provides an estimate of the cmc as ~ 0.1 mM, a parameter for which there is some uncertainty and variability in the literature (38, 39).

The impact of additives, such as NaCl, $MgCl_2$, $AlCl_3$ and citric acid, which affect headgroup interactions and pH, have little impact upon the saturation adsorption values. This is similar to that observed for escin as the pH was varied (12). Hence charge interactions have a minimal impact upon the packing and the saturation adsorption values. The addition of $MgCl_2$, $AlCl_3$ and citric acid, but not NaCl, result in an apparent and significant reduction in the cmc. This is similar to that observed for escin as the pH is increased from 4 to 8. This implies a specific interaction associated with the onset of micellisation, or that saturation adsorption occurs well before the onset of micellisation. The onset of gelation in the bulk is shown to have a minimal impact upon the adsorption, and confirms that the gelation mechanism in the bulk solution does not significantly affect the surface activity. It does, however, produce a rougher surface at the air-water interface, with a roughness over a length scale large compared to the neutron coherence length, and is consistent with a macroscopically wavier surface.

The SANS measurements show that GA forms globular elongated micellar structure, but relatively modest in size. This is broadly similar to that for escin and consistent with related observations in the literature (38, 38, 41, 42). The data show no evidence of longer rod-like or fibrillar structures. The

modest anisotropy in shape, which is well described by prolate ellipsoids, is confirmed by a lack of alignment under shear flow. The addition of electrolyte and citric acid, which promote gelation, result in only modest micellar growth. Comparison with the structure of escin, tea and Quillaja saponin micelles illustrate the importance of the details of the headgroup structure in determining the self-assembly properties. These preliminary structural measurements suggest that a more detailed structural study is justified, and that from which the general criteria for saponin self-assembly could be established.

ACKNOWLEDGEMENTS

The provision of beam time on the INTER and SANS2D neutron scattering instruments at the ISIS Neutron source is acknowledged. The invaluable scientific and technical assistance of the Instrument Scientists and support staff is greatly appreciated. IMT, AB, REP and SLH thank Innovate UK for funding under the Industrial Biology Catalyst scheme, grant number 131168, 'A synthetic biology-based approach to engineering triterpenoid saponins and optimisation of industrial applications'. JRPW acknowledges the support from the BBSRC grant BB/MO28968/1.

AUTHOR CONTRIBUTIONS

Al the authors have contributed to the different aspects of the paper, which include experimental design and measurements, analysis and interpretation of the data, preparation and editing of the manuscript, and management of resources: and specifically IMT, AB, REP, RKT, JP, PXL, JRPW, RW, JD have been involved in the measurements, interpretation of the data and experimental design. JRPW, SLH in the management of resources, and IMT, RKT, JP, PXL, JRPW, SLH in the editing of the manuscript.

DECLARATION OF COMPETING INTERESTS

The authors declare that they have no competing financial interests or personal relationship that could have appeared to have influenced the work reported in this paper.

FUNDING SOURCES

Funded through the beam time awarded at the STFC's ISIS Facility, and funding from Innovate UK under the Industrial Biology Catalyst scheme, grant number 131168, 'A synthetic biology based approach to engineering triterpenoid saponins and optimisation of industrial applications'.

SUPPLEMENTARY INFORMATION

Some supplementary data, in the form of tables and graphs, can be found online under Supplementary Information.

REFERENCES

(1) K Holmberg, Natural Surfactants, Curr. Opin. Coll. Int. Sci. 2002, 6, 148-159

(2) P Foley, A Kermanshahi Pour, ES Beach, JB Zimmerman, Derivation and synthesis of renewable surfactants, Chem. Soc. Rev. 2012, 41, 1499-1518

(3) RE Otzen, Biosurfactants and surfactants interacting with membranes and proteins, Biochim, Biophys. Acta, 2017, 1859. 639-649

(4) EZ Roz, E Rosenberg, Natural role of biosurfactants, Environ. Microbiol. 2001, 3, 229-236

(5) G Georgiou, SC Lin, MM Sharma, Surface active components from bioorganisms, Biotechnol. 1992, 10, 60-65

(6) JD Desai, IM Banat, Microbial production of surfactants and their commercial potential, Microbiol. Mol. Biol. Rev. 1997, 61, 47-64

(7) K Hoslettmann, A Marstrom, Saponins, Cambridge University Press, 1995

(8) JP Vicken, L Heng, A deGroot, H Gruppen, Saponins: classification and occurrence in the plant kingdom, Phytochemistry, 2007, 68, 275-297

(9) SG Sparg, ME Light, J van Standen, Biological activities and distribution of plant species, J. Ethnopharmacol. 2004, 94, 219-243

(10) O Guglu-Ustundaag, G Mazza, Spaonins: properties, applications and processing, Crit. Rev. Food Sci. Med. 2007, 47, 213-258

(11) D Oakenfull, Saponins in food: a review, Food Chem. 1981, 6, 19-40

(12) J Penfold, RK Thomas, I Tucker, JT Petkov, SD Stoyanov, N Denkov, K Golemanov, S Tcholakova, JRP Webster, Saponin adsorption at the air-water interface: neutron reflection and surface tension study, Langmuir, 2018, 34, 9540-9547

(13) K Wojciechowski, Surface activity of saponins from Quillaja bark at the air-water and oil-water interfaces, Coll. Surf. B, 2013, 108, 95-102

(14) V Ulaganathan. LD Castillo, JL Webber, TTM Ho, JK Ferri, M Krasowska, DA Beattie, The influence of pH on the interfacial behaviour of Quillaja bark saponin at the air-solution interface, Coll. Surf. B, 2019, 176, 412-419

(15) R Stanimorova, K Marinova, S Tcholakova, N D Denkov, SD Stoyanov, E Pelan, Surface rheology of saponin adsorbed layers, Langmuir, 2011, 27, 12486-12498

(16) K Golemanov, S Tcholakova, N Denkov, E Pelan, SD Stoyanov, Surface shear rheology of saponin adsorption layers, Langmuir, 2012, 28, 12071-12084

(17) K Golemanov, S Tcholakova, ND Denkov, E Pelan, SD Stoyanov, Remarkably high surface viscoelasticity of adsorption layers of triterpenoid saponins, Soft Matter, 2012, 9, 5738-5752

(18) N Pagureva, S Tcholakova, K Golemanov, N Denkov, E Pelan, SD Stoyanov, Surface properties of adsorption layers formed from triterpenoid and steroidal saponins, Coll. Surf. A, 2016, 491, 18-28

(19) PR Cheeke, Actual and potential applications of Yucca Schidigera and Quillaja Saponia saponins in human and animal nutrition, Proc. Am. Soc. Anim. Sci. 1999, E9, 1-10

(20) S Bottcher, S Drusch, Interfacial properties of saponin extracts and their impact on foam characteristics, Food Biophys. 2016, 11, 91-100

(21) KJ Jenkin, AS Atwall, Effects of dietry saponins on fecal bile acids and neutral steroids and availability of vitamins A and E in the chick, J. Nutr. Biochem. 1994, 5, 134-137

(22) F Sun, C Ye, K Thanki, D Leng, PM van Hassett, WE Hennink, CF van Nostrum, Mixed micellar systems stabilised with saponins for oral delivery of vitamin K, Coll. Surf. B, 2018, 170, 521-528

(23) J Liu, T Henkel, Traditional Chinese medicine (TCD): are polyphenols and saponins key ingredients triggering biological activity, Curr. Med. Chem. 2002, 9, 1483-1485

(24) N Fukada, H Tanaka, Y Shoyama, Isolation of the pharmacologically active saponin, ginzenoside Rb1 from Ginseng by immunoaffinity column chromatography, J. Nat. Prod. 2000, 62, 283-285

(25) C R Sirtori, Aescin: pharmacology, pharmokinetics and therapeutic profile, Pharmacol. Res. 2001, 44, 183-193

(26) R Brown, The natural way in cosmetics and skin care, Chem. Mark Rep. 1998, 254, FR8

(27) K Wojciechowski, M Orczyk, K Marcinkowski, T Kobrela, M Trupp, T Gutberlet, Effect of hydration of sugar groups on adsorption of Quillaja bark saponin at the air-water and silicon-water interfaces, Coll. Surf. B, 2014, 117, 60-67

(28) K Wojciechowski, M Orczyk, T Gutberlet, T Grue, Complexation of phospholipids and cholesterol by triterpenoic saponins in bulk and monolayers, Biochim. Biophys. Acta. Biomater. 2016, 1858, 363-373

(29) S Tsibranska, A Ivanova, S Tcholakova, N Denkov, Self-assembly of escin molecules at the air-water interface as studied by molecular dynamics, Langmuir, 2017, 33, 8330-8341

(30) J Tippel, M Lehmann, R von Klitzing, S Drusch, Interfacial properties of Quillaja saponins and its use for micellisation of leuten esters, Food Chem, 2016,212, 35-42

(31) S Mitra, S Dugan, Micellar properties of Quillaja saponin, 1. Effects of temperature, salt and pH on solution properties, J. Agric. Food Chem. 1997, 45, 1587-1595

(32) D Kitamoto, T Morita, T Fkuoka, M Konishi, T Imura, Self-assembly properties of glycolipid biosurfactant and their potential applications, Curr. Opin. Coll. Int. Sci. 2009, 4, 315-328

(33) D G Oakenfull, Aggregation of saponins and bile salts in aqueous solution, Aust. J. Chem. 1986, 39, 1671-1682

(34) C Dargel, R Geisler, Y Hannoppel, I Kember, N Sewald, T Hellweg, Self-assembly of the biosurfactant Aescin in solution: a SAXS and Fluorescence study, Coll. Int. 2019, 3, 47

(35) E Tykarski, S Sobiak, M Gdaniec, Supramolecular organisation of neutral and ionic forms of pharmaceutically relevant glycyrrhizic acid; amphiphile self-assembly and inclusion of small drug molecules, Crystal Growth Design, 2012, 12, 2133-2137

(36) MN Asl, H Hossenzadeh, Review of pharmological effects of glycyrrhiza sp and its bioactive compounds, Phytother. Res. 2008, 22, 709-724

(37) H Fujita, T Sakurai, M Yoshida, S Toyoshima, Anti-inflammatory effect of glycrrhizic acid, effect of glycyrrhizinic acid against carrageenan induced edema, uv-erythema, and skin sensitised with DNCB, Pharmacometrics, 1980, 19, 481-484

(38) M Kondo, H Minamino, G Obuyama, K Honda, H Nagasawa, Y otani, Physicochemical properties and applications of α- and β- glycyrrhizius, natural surface active agent in licorice root extract, J. Soc. Cosmet. Chem. 1986, 37, 177-189

(39) K Matsuoka, R Mitajima, Y Ishida, S Karasawa, T Yoshimura, Aggregate formation of gylcyrrhizic acid, Coll. Surf. A, 2016, 50, 112-117

(40) X He, J Dan, C Hong, Kinetics and thermodynamic studies of Glycyrrhizic acid and adsorption using S-8 macroporous resin, Asian J. Chem. 2013, 25, 9452-9456

(41) T Ralla, H Salminen, K Braun, M Eddmann, C Dawid, T Hoffmann, J Weiss, Investigation into the structure-function relationship of plant based glycyrrchizin: interfacial behaviour and emulsion formation, LWT, 2020, 129, 108910

(42) Z Wan, Y Sun, L Ma, J Guo, J Wang, S Yin, X Yang, Thermoresponsive structured emulsions based on fibrillary self-assembly of natural saponin glycyrrhizic acid, Food Funct. 2017, 8, 75-85

(43) JR Lu, RK Thomas, J Penfold, Surfactant layers at the air-water interface: structure and composition, Adv. Coll. Int. Sci. 2000, 54, 143-304

(44) J Penfold, Neutron scattering studies of micellar structure, Encyclopedia of surface and colloid science, 2002, 3653, Marcel Dekker, New York.

(45) IM Tucker, A Burley, RE Petkova, SL Hosking, J Penfold, RK Thomas, PX Li, JRP Webster, R Welbourn, Mixing natural and synthetic surfactants: coadsorption of triterpenoid saponins and sodium dodecyl sulfate at the air-water interface, Langmuir, 2020, 36, 5997-6006

(46) IM Tucker, A Burley, RE Petkova, SL Hosking, J Penfold, RK Thomas, PX Li, K Ma, JRP Webster, R Welbourn, Surfactant / biosurfactant mixing: adsorption of saponin / nonionic surfactant mixtures at the air-water interface, J. Coll. Int. Sci. 2020, 574, 385-392

(47) JRP Webster, S Holt, R Dalgleish, INTER: the chemical interfaces reflectometer on the second target station at ISIS, Phyisca B, 2006, 385-386, 1163-1166

(48) RK Heenan, SM King, DS Turner, JR Treadgold, SANS2D at the ISIS second target station, Proc. ICANS XVII, 2006, 780-785

(49) PG Cummins, EJ Staples, B Millen, J Penfold, A Couette shear flow cell for small angle neutron scattering, Meas. Sci. Technol. 1990, 1, 179-183

(50) J Penfold, EJ Staples, IM Tucker, GJT Tiddy, A Khan Lhodi, Shear induced structures in concentrated micellar phases, J. Appl. Cryst. 1997, 30, 744-749

(51) RK Heenan, SM King, R Osborn, HB Stanley, RAL Internal report, RAL-89-128, 1989

(52) JB Hayter, J Penfold, Determination of micelle structure and charge using neutron small angle scattering, Coll. Polym. Sci. 1983, 261, 1022-1030

(53) JB Hayter, J Penfold, An analytic structure factor for macroion solutions, Mol. Phys. 1981, 42, 109-118

(54) T Geisler, D A Weitz, Tracer microrheology in complex fluids, Curr. Opin. Cool. Int. Sci. 1998, 3, 586-592

(55) PX Li, ZX Li, HH Shen, RK Thomas, J Penfold, JR Lu, The use of the Gibbs equation to determine surface excesses of nonionic surfactants and polymers at the air-water interface, Langmuir, 2013, 29, 9324-9334

(56) H Xu, K Ma, PX Li RK Thomas, J Penfold, JR Lu, Limitations in the application of the Gibbs equation to anionic surfactants at the air-water interface: SDS and SLES above and below the cmc, Langmuir, 2013, 29, 9335-9351

(57) NM van Os, JR Haak, LAM Rupert, Physicochemical properties of selected anionic, cationic and nonionic surfactants, Elsevier, Amsterdam, 1993

(58) KL Steller, JF Scamehorn, Surfactant precipitation in aqueous solutions containing mixtures of anionic and nonionic surfactants, J. Am. Oil Chem. Soc. 1986, 63, 566-574

(59) RSS de Oliveira, NSM Huachaca, M Lemos, NT Santos, E Feitosa, LC Salay, Molecular interactions between pluronic F127 and saponins in aqueous solution, Coll. Polym, Sci. 2020, 298, 112-122

(60) JN Israelachvili, DJ Mitchell, BW Ninham, Theory of self-assembly of hydrocarbon amphiphiles into micelles and bilayers, J. Chem. Soc. Faraday Trans. 1976, 72, 1525-1568

GRAPHICAL ABSTRACT